Electronic Supplementary Material (ESI) for Lab on a Chip

Self-Powered Microfluidic Chips for Multiplexed Protein Assays from Whole Blood

Lidong Qin, Ophir Vermesh, Qihui Shi, and James R. Heath*

NanoSystems Biology Cancer Center(NSBCC), Kavli Nanoscience Institute, Division of Chemistry and Chemical Engineering, California Institute of Technology, Pasadena, California, 91125, USA. E-mail: heath@caltech.edu;Tel: 626-395-6079

1. Video clip 1 (Peroxide chip blood separation.avi). This real time movie is representative of a typical human blood assay. The movie shows how the air pressure that is generated in the H_2O_2 fuel reservoir is harnessed to separate plasma from whole blood. The blood is separated into two channels for the simultaneous analysis of proteins from both protein-spiked and non-spiked blood.
2. Video clip 2 (Flow speed variance.avi). This real time movie demonstrates the flow-speed variations that were designed into the various plasma channels, for generating the data shown in Fig. 5A. For this movie, blood cells are intentionally flowed through the 6 parallel variable width plasma channels to illustrate the correlation of flow rate with channel width. The slow flow of blood cells near the channel walls is consistent with the parabolic flow profile of fluids in microfluidic channels.
3. The barcode readout scheme that was utilized for this work. The assay scheme in this paper is similar to that described in our recent publication.[3] The readout scheme is shown in Fig. S1. A set of ssDNA oligomers are first patterned onto polylysine glass slides using the technique of microfluidic-guided flow-through patterning (Fig. S1A).[3] This forms the barcode, with each barcode stripe containing a unique ssDNA oligomer. The automated IBBC chip is then assembled, and is ready for priming. During the priming step, 1° antibodies conjugated with complementary ssDNA' oligomers (Fig. 1B) are flowed through the plasma skimming channels, and this converts the ssDNA barcodes into antibody barcodes via DNA hybridization. In the assay step, the protein biomarkers from the plasma samples, if present, bind to the antibody barcodes. In the readout step, all relevant biotinylated 2° antibodies are flowed through the plasma channels, and then straptavidin-Cy5 fluorescent labels are added to develop the assay (Fig. S1B). Reagents used are listed in Table S1.

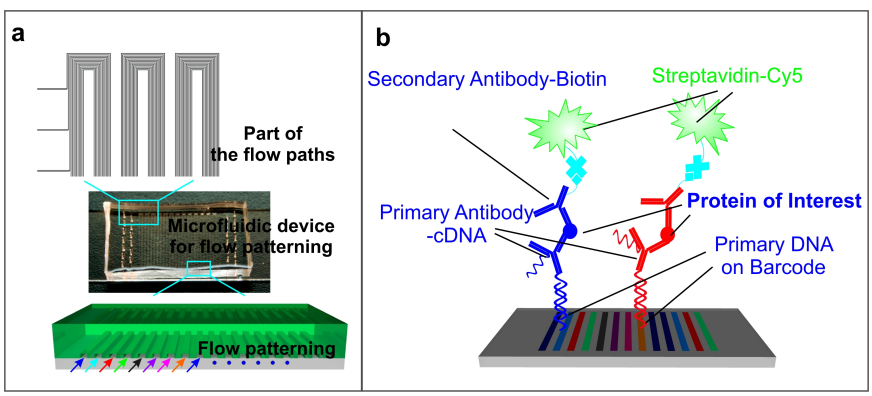

Fig. S1. DEAL bar code assay platform. A. Flow patterning of primary DNA oligos. B. Binding scheme of the immunoassay on a bar code DNA pattern.

Table S1. Reagents used for the protein biomarker barcodes.

Bar code #	Protein	ssDNA oligomers and (complementary) ssDNA' oligomers	
1	Complement component 3 (C3)	5'-AAA AAA AAA AGA GTA GCC TTC CCG AGC ATT-3'	5' NH3-AAA AAA AAA AAA TGC TCG GGA AGG CTA CTC-3'
2	Fibrinogen	5'-AAA AAA AAA ATA TGG GTC TTG CTG ATA CGC	5' NH3-AAA AAA AAA AGC GTA TCA GCA AGA CCC ATA-3'
3	C-reactive protein (CRP)	5'-AAA AAA AAA AGC GTG TGT GGA CTC TCT CTA-3'	5' NH3-AAA AAA AAA ATA GAG AGA GTC CAC ACA CGC-3'
4	Plasminogen	5'-AAA AAA AAA ATC GCC GTT GGT CTG TAT GCA-3'	5' NH3-AAA AAA AAA ATG CAT ACA GAC CAA CGG CGA-3'
5	Interleukin (IL)12	5'-AAA AAA AAA AGG CGG CTA TTG ACG AAC TCT-3'	5' NH3-AAA AAA AAA AAG AGT TCG TCA ATA GCC GCC-3'
6	IL17A	5'-AAA AAA AAA AAA TGA GCG CGA ACA CCT GAC-3'	5' NH3-AAA AAA AAA AAA TGA GCG CGA ACA CCT GAC-3'
7	Tumor necrosis factor-alpha (TNFα)	5'-AAA AAA AAA ATC TTC TAG TTG TCG AGC AGG-3'	5' NH3-AAA AAA AAA ACC TGC TCG ACA ACT AGA AGA-3'
8	IL13	5'-AAA AAA AAA AGC GTG TGT GGA CTC TCT CTA-3'	5' NH3-AAA AAA AAA ATA GAG AGA GTC CAC ACA CGC-3'
9	IL8	5'-AAA AAA AAA ACT CTG TGA ACT GTC ATC GGT-3'	5' NH3-AAA AAA AAA AAC CGA TGA CAG TTC ACA GAG-3'
10	IL2	5'-AAA AAA AAA AGT CCT CGC TTC GTC TAT GAG-3'	5' NH3-AAA AAA AAA ACT CAT AGA CGA AGC GAG GAC-3'
11	Control	5'-AAA AAA AAA AGT CGA GGA TTC TGA ACC TGT-3'	
12	IL10	5'-AAA AAA AAA ATA ATC TAA TTC TGG TCG CGG-3'	5' NH3-AAA AAA AAA ACC GCG ACC AGA ATT AGA TTA-3'
13	IL6	5'-AAA AAA AAA ATG CCC TAT TGT TGC GTC GGA-3'	5' NH3-AAA AAA AAA ATC CGA CGC AAC AAT AGG GCA-3'

4. The channel depth is ~11 μm on average. A topography image was attached herein to demonstrate the dimensions of the plasma skimming channel. Channels were rounded on purpose to favor blood separation. (Figure S2)

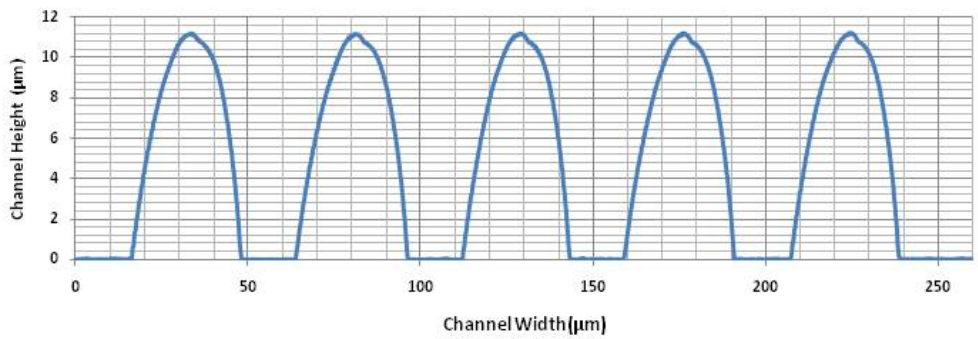

Fig. S2: Height profile of plasma skimming channels in the device mold. The height is about 11 μm on average.

5. The sub-channels of six different widths are elongated in comparison to the original single width plasma channel. (Figure S3) The purpose of lengthening these channels is to increase the flow resistance difference between the six sub-channels. The channel height profile is also measured, which clarifies the dimension of the six sub-channels.

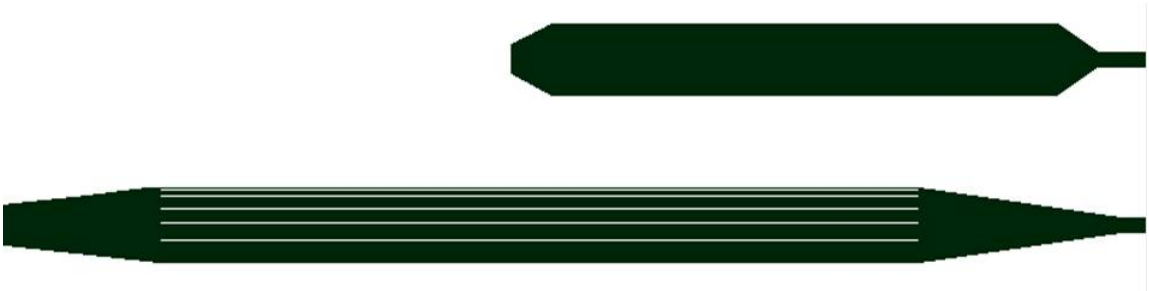

Fig. S3. Plasma channel length of the six sub-channels in the variable flow rate experiment, in comparison to the original single plasma channel. The length is elongated from 5 mm to 7.5 mm.

The dimensions of the sub-channels are now characterized by a height profile scan, Figure S4. Besides the width variance, which is about 1x, 2x, 6x, 8x, 10x, and 15x from the narrowest to the broadest, there is a slight height variance that results during the photoresist development step in the fabrication process. . The channels were also rounded during fabrication. When designing the device, we used Darcy's Law to calculate the flow rate variance, which gives flow rate variances of 1x, 2x, 6x, 8x, 10x, and 15x, but the real flow rate is still related to the channel material, roughness, and other factors. Video clip 2 demonstrates that the channel dimensions control the flow rate.

Approaches to optimizing assays for fast measurements have been extensively discussed in reference 32 in our manuscript (M. Zimmermann et al, *Biomedical Microdevices*, 2005, **7**, 99-110). The strategy for rapid assays is to have a high fluid flow velocity to prevent mass transport limitations and a small protein capture area to increase analyte exploitation. Because the flow profile of fluid in a microfluidic channel is parabolic, the flow of analytes carried in these fluids is likewise parabolic , and this can influence the results. For relatively low flow rates, the assays of Figure 5D reflect these velocity profiles, but for saturated assays, the effect is absent. Moreover, the parabolic flow profile likely also explains the slow flow of blood cells near the channel wall.

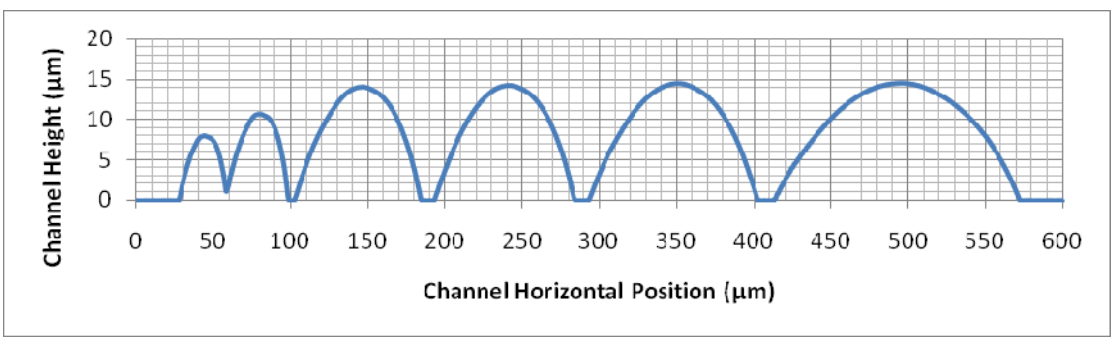

Fig. S4. Height profile of plasma skimming channels in a device mold.